University of California at Santa Cruz

Muon Physics

PHYS 134 Lab Report

by

Jacob Shearer

Instructor: Sasha Sher

Abstract

In the experiment detailed in this report, a scintillator was used to determine the average lifetime of the muon. Muons produced in the upper atmosphere enter the scintillator and excite its constituent atoms, which eventually become de-excited and emit a pulse of light. When the muon itself decays, a second pulse is also produced. These two pulses are detected and converted into electrical signals by a photomultiplier tube, and the interval between these two signals is then measured by a computer and recorded. Many thousands of these decays are accumulated and the average lifetime of the muon is determined by fitting these decays to a distribution. This lifetime is then used to determine the Fermi coupling constant. The lifetime of the muon was determined to be 2.04 ± 0.03 microseconds, and the reduced Fermi coupling constant was determined to be $1.21 \times 10^{-5} \pm 5.02 \times 10^{-8}$ GeV^{-2}.

Contents

List of Figures **iv**

List of Tables **vi**

1 Introduction **1**

1.1 Background 2

2 Methods **7**

2.1 Description of Apparatus 7

2.2 Calibration of the Apparatus 9

2.3 Measurement of the FPGA's Timing Properties 10

2.4 Measuring Muon Decays 11

2.5 Data Analysis 12

2.5.1 Analysis of the FPGA's Linearity 12

2.5.2 Calculating the Muon's Lifetime 12

2.5.3 Calculating the Fermi Coupling Constant 14

3 Results **16**

4 Discussion **21**

5 Bibliography **24**

List of Figures

1.1 A diagram depicting the interaction between cosmic rays and the molecules of the upper atmosphere, producing pions which eventually decay into muons. Image borrowed and modified slightly from Thomas Coan and Jingbo Ye's Muon Physics experiment manual. . . . . (3)

2.1 A diagram of the experimental apparatus. Taken from Thomas Coan and Jingbo Ye's Muon physics experiment manual. . . . . (7)

2.2 A picture of amplifier and discriminator outputs as viewed via an oscilloscope. The discriminator output, pictured in yellow, is roughly a trough function, and the amplifier output, pictured in blue, is a function with a single peak. When the discriminator threshold is increased, the taper of the discriminator becomes less and less narrow and the amplitude of the amplifier output increases. . . . . (8)

2.3 The amplifier and discriminator outputs observed with the pulser active. Two signals can be seen, each corresponding to one of the pulses in the pair produced by the pulser. The two time cursors (the vertical yellow dotted lines) are aligned with the rising edges of the peaks so that the time between consecutive pulses can be measured. . . . . (10)

3.1 A plot of the average interval measured by the FPGA vs. the interval measured by the oscilloscope with pulser intervals varying from 2 microseconds to 20 microseconds. The trendline (shown in orange) indicates a linear relationship. Error bars are shown in red. . . . . (17)

3.2 A histogram of the first trial's data along with its corresponding fit line (depicted in red. Uncertainties for each bin are displayed via the orange error bars. . . . . (18)

3.3 A histogram of the second trial's data along with its corresponding fit line (depicted in red). Uncertainties for each bin are displayed via the orange error bars. . . . . (19)

List of Tables

3.1 A summary of the intervals measured by the oscilloscope and FPGA, as well as the uncertainties of the FPGA measurements, taken with the pulser. . . . . (16)

1

Introduction

Muons are one of the fundamental particles described by the standard model of particle physics. They are one of the six members of the lepton family (of which the other five are tauons, electrons, and their associated neutrinos), meaning that they only interact with other particles via the weak and electromagnetic forces. Most of the muons encountered on Earth are produced when cosmic rays interact with the molecules of the upper atmosphere, which produces a shower of particles including charged pions. These charged pions eventually decay into muons along with their corresponding muon neutrino or antineutrino. Muons produced this way typically have very high kinetic energy, and thus travel some distance before finally decaying themselves.

The experiment detailed in this report seeks to measure the lifetime of the muon using a scintillator, which can detect the decays of muons and other particles. Using the scintillator and several other electrical components which are described with more detail in the “Methods” section, many thousands of such decays are recorded. These are then sifted into “muon decay-like” events with the aid of a computer program and subsequently used in a least squares fit for the distribution of muon lifetimes. From this fit, the average lifetime of $\mu^{\pm}$ is determined.

Once determined, the lifetime of the muon, aside from being of interest in its own right, can be used to determine the Fermi coupling constant, a measure of the strength of the weak force. Additionally, a comparison of the measured lifetime with the calculated travel time of the muons from the site of their creation high in the atmosphere to sea level provides qualitative evidence for relativistic time dilation.

1.1 Background

Cosmic rays produced in interstellar space regularly interact with molecules in the Earth's upper atmosphere. These rays, which are primarily composed of protons, collide with the nuclei of atmospheric molecules, which produces a shower of subatomic particles. Several different species of particles are produced, but the most interesting for our purposes are positively and negatively charged pions. Many of the pions produced eventually undergo spontaneous decay via the weak force. The decays of positive and negatively charged pions are described by Equations 1.1 and 1.2 respectively.

$$\pi^{+} \rightarrow \mu^{+} + \nu_{\mu} \tag{1.1}$$

$$\pi^{-} \rightarrow \mu^{-} + \overline{\nu}_{\mu} \tag{1.2}$$

As these equations show, a charged pion decays into a muon of the same charge along with either a muon neutrino, in the case of a positively charged muon, or a muon antineutrino, in the case of a negatively charged muon. Figure 1.1, presented below, summarizes this process (Coan & Ye, 2005, pp. 3-4).

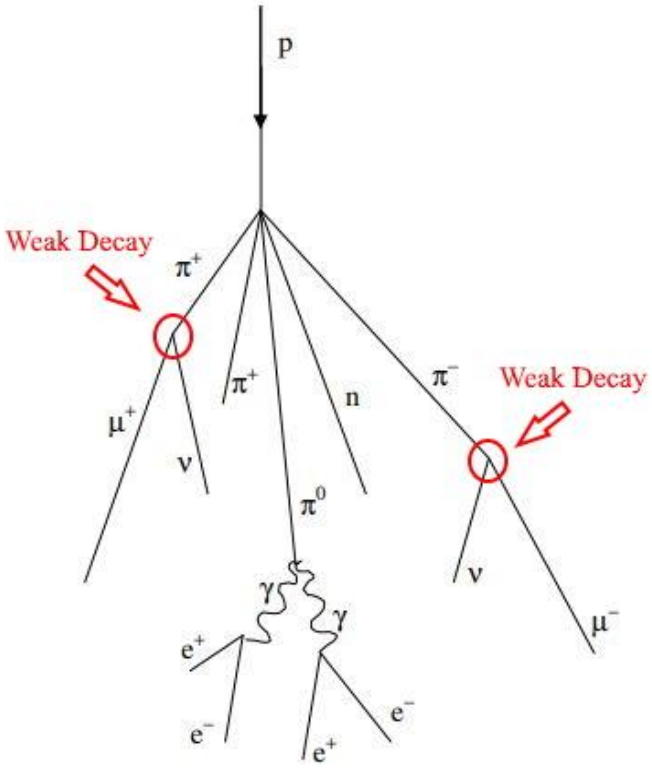

Figure 1.1: A diagram depicting the interaction between cosmic rays and the molecules of the upper atmosphere, producing pions which eventually decay into muons. Image borrowed and modified slightly from Thomas Coan and Jingbo Ye's Muon Physics experiment manual.

The muons produced by this decay, which occurs about 15 kilometers above sea level, typically have quite high kinetic energy, enabling them to move at relativistic speeds and, thus, travel quite long distances. Though they lose some of this kinetic energy as they travel, approximately 170 muons per square meter make it all the way to sea level every second, each with an average energy of 4 GeV (Brown, 2022, p. 39). This experiment was conducted in a laboratory very close to sea level (approximately 300 meters above), so the flux and average energy of the muons detected by the scintillator are expected to be in the vicinity of these values.

Muons are unstable particles, and thus decay after a short period of time. The decays of positively-charged and negatively charged muons are described by Equations 1.3 and 1.4 respectively.

$$\mu^+ \rightarrow e^+ + \nu_e + \overline{\nu}_\mu \tag{1.3}$$

$$\mu^- \rightarrow e^- + \overline{\nu}_e + \nu_\mu \tag{1.4}$$

The scintillator medium used to detect these decays is composed of a combination between a plastic solvent and one or more fluors. As a muon enters the scintillator, it loses some of its kinetic energy, exciting or ionizing some of the atoms of the solvent. A portion of this energy is then transferred to the fluor molecules, which excites their constituent atoms as well. When these atoms' electrons jump down to lower energy states, they emit light, which constitutes the first light pulse (Coan & Ye, 2005, pp. 5-6).

After the muon enters the scintillator it continues for a short time before finally coming to a stop and decaying according to Equations 1.3 and 1.4. Because it has a quite small mass compared to that of the muon itself, the electron or positron produced during this decay is typically very energetic and thus continues on a path that takes it out of the scintillator. As it moves along this path, it interacts with the scintillator medium via the coulomb force, exciting the medium's atoms much like the muon itself did. As before, these atoms emit light upon becoming de-excited, and this constitutes the second light pulse (Coan & Ye, 2005, p. 6).

Although this mode of decay and process of detection is available to both negatively charged and positively charged muons, negatively charged muons also have an additional decay mode available to them: muon capture. Negatively charged muons behave much like heavy, unstable electrons, which allows them to bind to the atoms of the scintillator medium much like electrons. Those muons which get close enough to the nuclei of these atoms can be captured by

one of their protons, converting the proton into a neutron and emitting a muon neutrino, as shown by Equation 1.5 (Coan & Ye, 2005, p. 7).

$$\mu^- + p \rightarrow n + \nu_\mu \quad (1.5)$$

This interaction sometimes produces a photon as well, which, in the case of negative muons decaying via this mode, constitutes the second light pulse.

Both the first light pulse and the second pulse are detected and converted into an electrical signal by a photomultiplier tube, which is then sent to a timing clock. The first pulse starts the clock, the second pulse stops it, and the interval determined by the clock is then recorded by a computer. Thousands of such decay events are recorded and the distribution of the decay times is examined to determine the lifetime of the muon. Because the instrument has no way to distinguish between the decay of a positively charged muon and a negatively charged muon, this lifetime will be an average of positive and negative muon lifetimes (Coan & Ye, 2005, p. 9).

As discussed above, most of the muons detected by the scintillator are produced at a much greater altitude than the scintillator itself, meaning that many of the muons have already lived for some time before their decays are actually detected. However, the decay events detected by the scintillator are still distributed around the average muon lifetime according to the particle decay function (Coan & Ye, 2005, p. 5). This function is given by Equation 1.5:

$$N(t) = Ae^{-\frac{t}{\tau}} + B \quad (1.6)$$

where N is equal to the number of muons with decay time t, A is the initial number of muons entering the scintillator, B is the constant background arising from accidental double pulses, and τ is the average muon lifetime (Brown, 2022, p. 39). The parameters A and B, as well as τ, are

determined by organizing the decay events into bins and using the values of these bins in a least squares fit.

Because muons decay via the weak force, τ can be used to determine the Fermi coupling constant, G_F, which is a measure of the strength of the weak force. τ and G_F are related by Equation 1.7, shown below

$$\tau = \frac{192\pi^2\hbar^7}{G_F m_\mu^5 c^4} \tag{1.7}$$

where ħ is the reduced Planck's constant, m_μ is the mass of a muon, and c is the speed of light (Coan & Ye, 2005, p. 10).

2

Methods

The average muon lifetime was determined using a plastic scintillator and several other electronic devices. After the whole apparatus was properly calibrated, it was allowed to sit and record data for several days. This raw data was sifted for "muon-like" events and was subsequently analyzed to determine the lifetime. From this, the Fermi coupling constant was calculated.

2.1 Description of Apparatus

Figure 2.1, presented below, depicts a diagram of the apparatus used for the experiment.

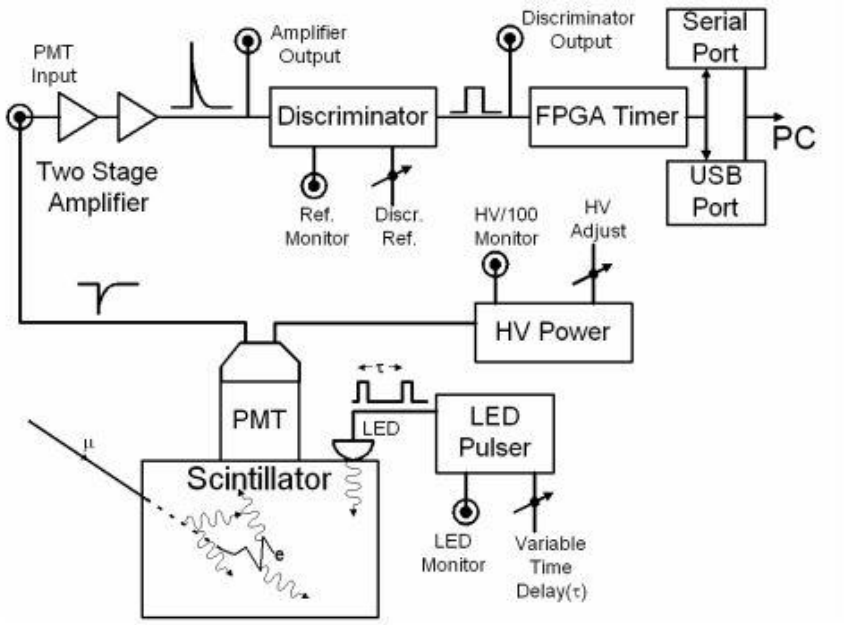

Figure 2.1: A diagram of the experimental apparatus. Taken from Thomas Coan and Jingbo Ye's Muon physics experiment manual (Coan & Ye, 2005, p. 15).

The scintillator medium is a combination of a plastic solvent and one or several fluors, and the scintillator itself is a right circular cylinder with a 15 cm diameter and 12.5 cm height that is made out of a transparent organic plastic. This is placed at the bottom of a tube made of black anodized aluminum alloy. Light pulses produced in the scintillator via the methods discussed in the introduction are first detected and converted into electrical signals by the photomultiplier tube. These signals are then passed through the amplifier, which amplifies them, before next being passed through the discriminator, which only lets signals that are greater than a certain threshold voltage pass.

Signals that make it through are then passed to the FPGA timer, which measures the interval between two consecutive signals (i.e. the decay time for a muon, where the first signal is the muon entering the scintillator and the second signal is the muon decaying). Finally, the FPGA communicates the measured interval to a personal computer via a USB connection, and these intervals are recorded using a computer program.

In addition to the components shown above, an oscilloscope is also connected to both the amplifier and the discriminator so that their respective outputs can be monitored. The discriminator is connected the oscilloscope's first channel, the amplifier is connected to the oscilloscope's second channel, and both inputs are terminated through a 50 Ω load. An example of the amplifier and discriminator output seen on the oscilloscope is presented below.

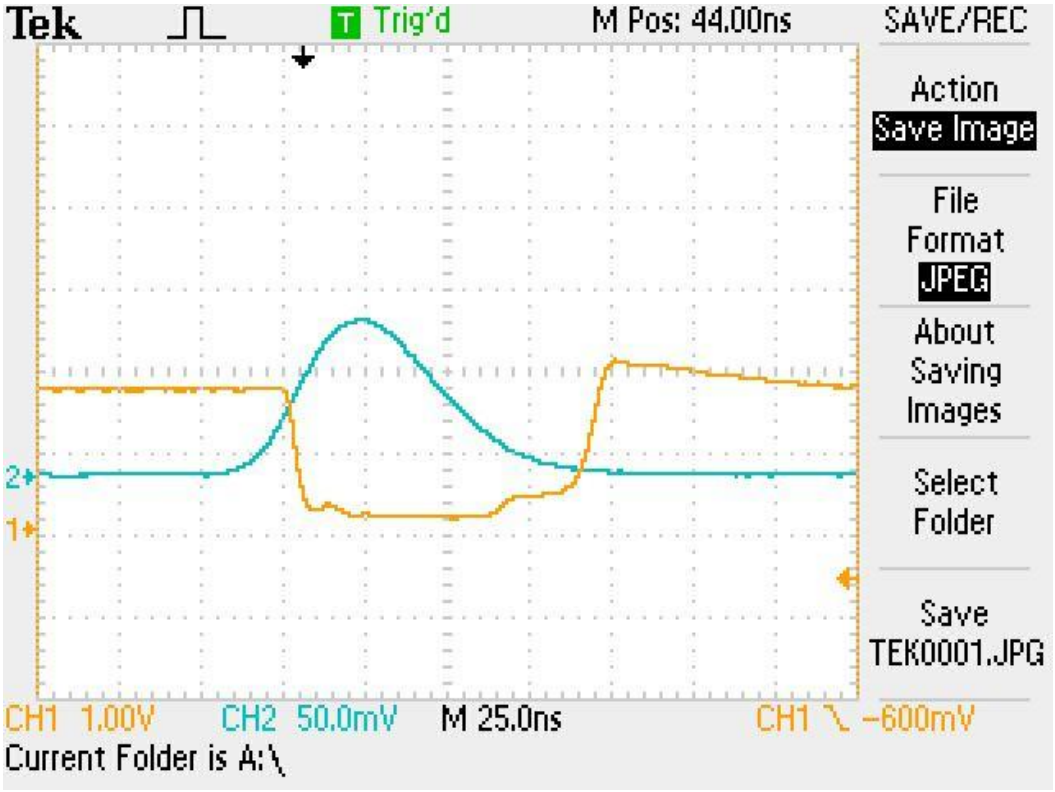

Figure 2.2: A picture of amplifier and discriminator outputs as viewed via an oscilloscope. The discriminator output, pictured in yellow, is roughly a trough function, and the amplifier output, pictured in blue, is a function with a single peak. When the discriminator threshold is increased, the taper of the discriminator becomes less and less narrow and the amplitude of the amplifier output increases.

2.2 Calibration of the Apparatus

In order to get good signals (i.e. signals without large amounts of random electronic noise), the discriminator's threshold voltage was set to be between 180 - 220 mV using the discriminator's threshold adjustment knob. Knowing that signals from the combination of the PMT and the amplifier needed to be within or above this range, the high voltage through the PMT was set to be between -1100 and -1200 V. The exact voltages used for both the discriminator and the PMT are featured in the "Results" section of this report.

2.3 Measurement of the FPGA's Timing Properties

Before measuring real decay events, it was necessary to establish the timing capabilities of the FPGA. This was primarily done using the detector's pulser, which is essentially just a circuit that produces pairs of light pulses inside of the scintillator using an LED.

First, the linearity of the FPGA was established by comparing interval measurements made by the FPGA with those made by an oscilloscope. The oscilloscope's cursors (set to "time" mode) were adjusted until the desired interval was reached, and the interval of the pulser was adjusted until the rising edges of the two pulses were aligned with the cursors. Figure 2.3, presented below, illustrates this.

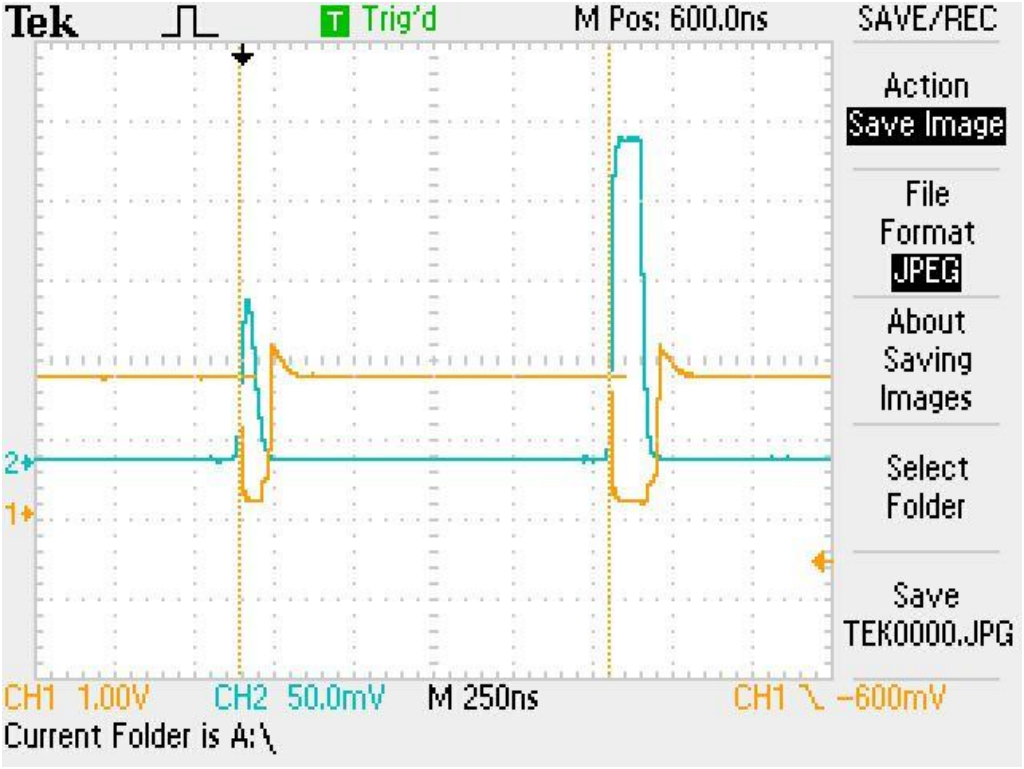

Figure 2.3: The amplifier and discriminator outputs observed with the pulser active. Two signals can be seen, each corresponding to one of the pulses in the pair produced by the pulser. The two time cursors (the vertical yellow dotted lines) are aligned with the rising edges of the peaks so that the time between consecutive pulses can be measured.

Once the desired pulser interval was achieved, the computer program responsible for recording measurements from the FPGA was used to record 10 pulse pair intervals. The resulting intervals were averaged, and this average was compared to the interval measured by the oscilloscope. This was done over a set of intervals ranging from 2 microseconds to 20 microseconds, in 2 microsecond steps, from which a plot of the FPGA intervals vs. the oscilloscope intervals was made. This plot, as well as the measured FPGA intervals, are presented in the "Results" section.

Second, the maximum possible time interval that the FPGA could measure was established. This was done by increasing the interval of the pulser until the FPGA effectively stopped recording results, shown in the computer program by a single entry in the raw data file corresponding to the number of events that "maxed out" the FPGA's timing capabilities. Once the pulser interval reached this point, the largest time interval recorded was taken to be the FPGA's maximum.

Finally, the FPGA's minimum observable time interval was determined. This was done by decreasing the interval of the pulser until it was effectively zero, and then taking the smallest interval recorded by the computer program to be the minimum.

2.4 Measuring Muon Decays

Measurement of decay events was accomplished by simply letting the apparatus run for a period of several days. Each event that occurred, including those that maxed out the FPGA's timing capabilities, was recorded by the computer program. Once data collection was complete, a list of each event's corresponding time interval was exported by the program. In order to determine the presence of any systematic error, a total of two of these trials were conducted and their final results were compared. Each trial lasted approximately two days.

2.5 Data Analysis

2.5.1 Analysis of the FPGA's Linearity

Once the pulser was calibrated to the desired interval, a total of 10 FPGA intervals were recorded using the computer program, and these 10 intervals were then averaged to get a single value. The uncertainty in this average value was computed using the following equations:

$$\sigma_i^2 = \frac{1}{9}\sum_{n=1}^{10}(\bar{i} - i_n)^2 \tag{2.1}$$

$$\sigma_{\bar{i}} = \frac{\sigma_i^2}{\sqrt{10}} \tag{2.2}$$

where the variable $\bar{i}$ represents the average interval length, and i_n represents one of the 10 intervals. These were used to calculate the variance described by Equation 2.1, which was in turn used to calculate the final uncertainty in the average interval via Equation 2.2.

This procedure was repeated a total of 10 times, yielding 10 average FPGA intervals and their uncertainties, along with 10 intervals measured by the oscilloscope. A scatterplot of the FPGA intervals vs. the oscilloscope intervals was made using the numpy method scatter, and a trendline of the resulting plot was made using the numpy method polyfit. The uncertainties in the FPGA intervals were captured in the plot via a set of vertical error bars, one for each plot point.

2.5.2 Calculating the Muon's Lifetime

Before the raw data could be analyzed, it was necessary to first sift the data for muon decay-like events. A simple program was used to remove events from the data that were greater than 20 microseconds, including those that maxed out the FPGA's timing capabilities. After being sifted, the remaining events were sorted and put into 100 bins of equal width ranging from zero microseconds to 20 microseconds. The uncertainty in the number of muon decays in each bin is given by Equation 2.3, where N is the number of muon decays in the bin.

$$\sigma_N = \sqrt{N} \tag{2.3}$$

The bins which were populated, as well as their corresponding calculated uncertainties, were then fed into scipy's optimize curve fit method along with Equation 1.6 to obtain values for the parameters A, B, and, most importantly, τ. The uncertainties in each of these parameters were determined from the covariance matrix returned by scipy optimize, which contained the parameters' variances in its diagonal entries. Extracting these entries and taking their square roots yielded the final uncertainties.

To determine the accuracy of the fit and, thus, the significance of the data, a chi-squared test and a p-test were conducted. Equations 2.4 and 2.5 describe the functions used for the chi-squared test.

$$\chi^2 = \sum \frac{(N_{measured} - N_{fit})^2}{\sigma_N^2} \tag{2.4}$$

$$Reduced\,\chi^2 = \frac{\chi^2}{v} \tag{2.5}$$

The variable $N_{measured}$ corresponds to the measured number of muons inside of a given bin and the variable N_{fit} corresponds to the number of muons as given by Equation 1.6 evaluated at the time corresponding to the central value of the bin. The variable v corresponds to the number of

degrees of freedom, of which there were a maximum of 97 (accounting for 100 bins and 3 fitting parameters). Bins which contained no events were not used when determining the fitting parameters in order to avoid divide-by-zero errors, so the value of v varied depending on the number of unpopulated bins which were excluded. Once a value for chi-squared had been determined, it was used in conjunction with scipy's cumulative distribution function method to obtain the p-score for the fit. A significance level of 5% (p = 0.05) was used in this analysis.

All of these steps were repeated for both of the two trials, and once a value for τ had been determined for each, the two τ values were averaged to obtain the final value of τ. The uncertainty in this value was obtained via Equation 2.6, which was obtained using error propagation. σ_{τ_1} is the uncertainty in the first trial's τ value, and σ_{τ_2} is the uncertainty in the second trial's τ value.

$$\sigma_{\tau} = \frac{\sqrt{\sigma_{\tau_1} + \sigma_{\tau_2}}}{2} \tag{2.5}$$

This value was then compared to the accepted value for the lifetime of a muon using the percent difference formula.

2.5.3 Calculating the Fermi Coupling Constant

Solving Equation 1.7 for G_F and manipulating it somewhat results in Equation 2.7, the reduced Fermi coupling constant, $G_F^{\,o}$.

$$G_F^{\,o} = \frac{G_F}{(\hbar c)^3} = \sqrt{\frac{192\pi^3\hbar}{\tau(m_\mu c^2)^5}} \tag{2.7}$$

The uncertainty in this value, in terms of the uncertainty in τ, σ_τ, can be obtained using the error propagation formula described by Equation 2.8.

$$\sigma_{G_F^{\,o}} = \sqrt{\left(\frac{dG_F^{\,o}}{d\tau}\sigma_\tau\right)^2} \tag{2.8}$$

Evaluating the derivative and simplifying yields Equation 2.9.

$$\sigma_{G_F^{\,o}} = \sqrt{\frac{12\pi^3\hbar\sigma_\tau}{\tau^3(m_\mu c^2)^5}} \tag{2.9}$$

The calculated value for the reduced Fermi coupling constant is then compared with its accepted value using the percent difference formula.

3

Results

Both trials, as well as the measurement of the FPGA's timing properties, were conducted with a discriminator threshold voltage of 220 mV and with a high voltage of -1113 Volts through the photomultiplier tube.

Measurement of the FPGA's timing properties was conducted according to the procedure described in "Methods," and it was determined that the FPGA had a minimum measurable interval of 0.62 microseconds and a maximum measurable interval of 19.974 microseconds. Table 3.1, presented below, summarizes the pulser intervals as measured by the oscilloscope, the average pulser intervals as measured by the FPGA, and the uncertainty on the FPGA's measurements.

Oscilloscope Intervals (μs)	2	4	6	8	10	12	14	16	18	20
FPGA Intervals (μs)	2.002	3.83	5.838	7.828	9.838	11.918	14.01	16	17.982	19.974

FPGA Uncertainties (μs)	0.008	0.008	0.008	0.008	0.008	0.008	0.008	0.008	0.008	0.008

Table 3.1: A summary of the intervals measured by the oscilloscope and FPGA, as well as the uncertainties of the FPGA measurements, taken with the pulser.
Additionally, Figure 3.1, presented below, plots the tabulated data.

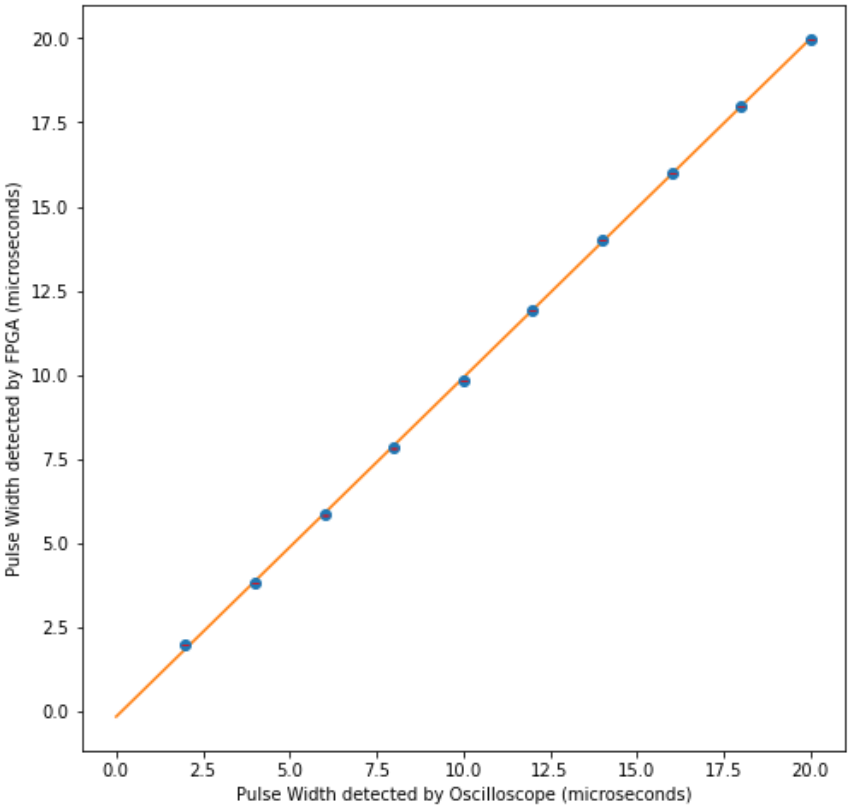

Figure 3.1: A plot of the average interval measured by the FPGA vs. the interval measured by the oscilloscope with pulser intervals varying from 2 microseconds to 20 microseconds. The trendline (shown in orange) indicates a linear relationship. Error bars are shown in red.

As the figure shows, the FPGA responds linearly with the oscilloscope, and therefore with corresponding increases in the pulser interval. This result verifies that any intervals measured by the FPGA are quite accurate, as long as those intervals occur within the FPGA's minimum and maximum measurable interval thresholds.

Moving on to the primary experiment, exactly 3000 muon decays were detected by the scintillator during the first trial. Figure 3.2, presented below, depicts a histogram of the binned data along with the fitline created using the data.

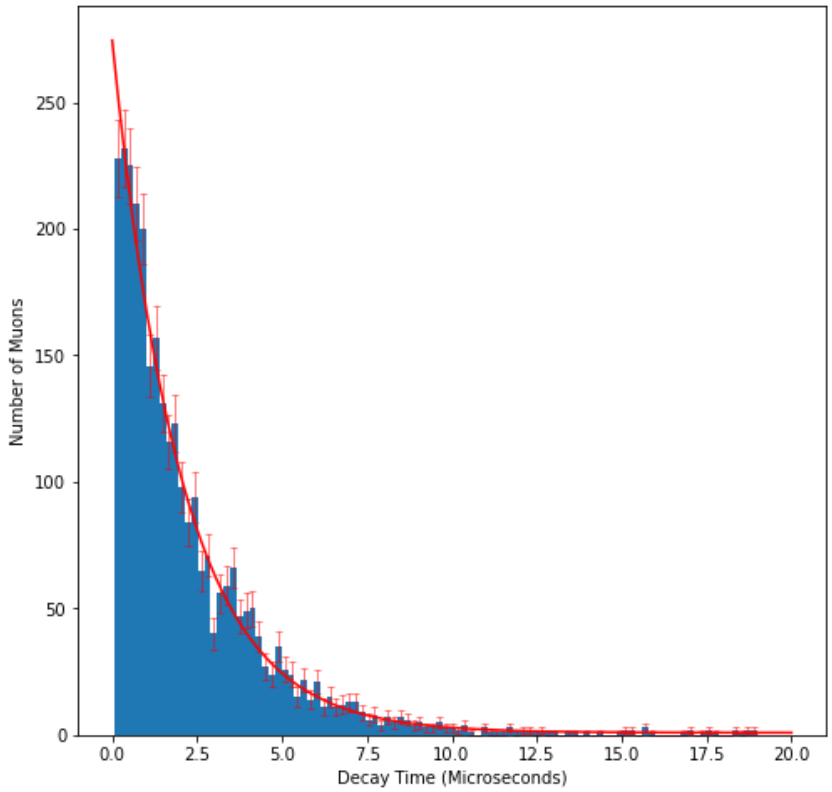

Figure 3.2: A histogram of the first trial's data along with its corresponding fit line (depicted in red). Uncertainties for each bin are displayed via the orange error bars.

The fitting parameters used to create the fitline, including this trial's τ, are given below with their corresponding uncertainties. The parameters A and B are explained in the Introduction.

$A = 273.61483 \pm 7.79097\ muons$

$B = 0.87173 \pm 0.21722\ background\ events$

$\tau = 2.03867 \pm 0.04808\ microseconds$

Additionally, the chi-squared, reduced chi-squared, and p-test values for the fit are given below.

$\chi^2 = 70.03961$

$Reduced\ \chi^2 = 0.84385$

$P\ value = 0.844029$

The reduced chi-squared and p value were calculated with 83 degrees of freedom, meaning that 14 unpopulated bins were removed when calculating the fit. The chi-squared and reduced chi-squared values are both below the number of degrees of freedom and one, respectively, indicating that the fit is very good. Additionally, the p value is significantly higher than the confidence level of 0.05, indicating that this result is statistically significant. Thus, this value of τ is acceptable.

During the second trial 3240 muon decays were detected by the scintillator. Just as with the first, this data was binned and used to determine a fitline. Figure 3.3 depicts a histogram of this data and its corresponding fitline.

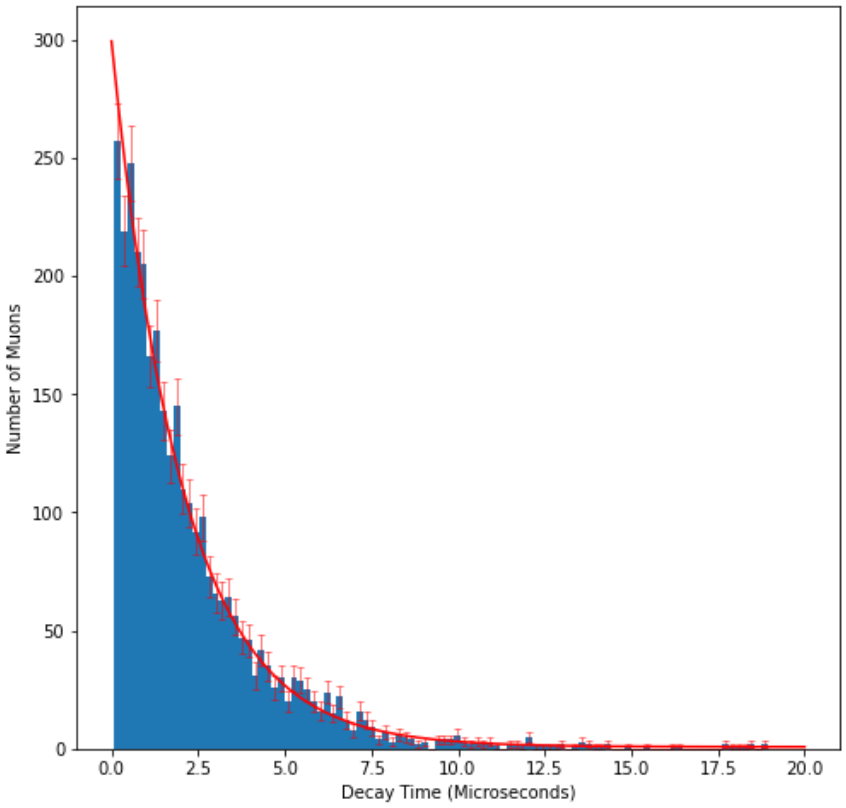

Figure 3.3: A histogram of the second trial's data along with its corresponding fit line (depicted in red). Uncertainties for each bin are displayed via the orange error bars.

The second trial's fitting parameters and τ value are given below.

$A = 298.65379 \pm 7.79097\ muons$

$B = 0.75904 \pm 0.21722\ background\ events$

$\tau = 2.04908 \pm 0.04808\ microseconds$

The chi-squared, reduced chi-squared, and p-test values for the second trial fit are given below.

$\chi^2 = 64.58159$

$Reduced\ \chi^2 = 0.84385$

$P\ value = 0.89504$

In this case, the reduced chi-squared and p value were calculated using 80 degrees of freedom, meaning that a total of 17 unpopulated bins were not included in the fit calculation. Once again, the chi-squared and reduced chi-squared values indicate a good fit, and the p value is well above 0.05, indicating that this result is statistically significant. Therefore, this value of τ, is also acceptable.

Using the two values of τ obtained from each trial, the final value of τ was calculated by taking their average as well as the average of their uncertainties.

$\tau = 2.04387 \pm 0.03399\ microseconds$

Using this value of τ and its uncertainty with Equations 2.6 and 2.8, the final value for the reduced Fermi coupling constant was calculated and is presented below.

$G_F^{\ o} = 1.20658 \times 10^{-5} \pm 5.01767 \times 10^{-8}\ GeV^{-2}$

This value was obtained using a muon rest mass of 0.10566 GeV/c^2 (Zyla et al., 2021).

4

Discussion

Through the measurement of several thousand muon decays over the course of two trials, the average lifetime of a muon was determined to be 2.04387 ± 0.03399 microseconds. This final

value, as well as its uncertainty, was determined by averaging the τ values obtained from each trial (featured in Results). This final τ value was then used to calculate the Fermi coupling constant, $G_F^{\,o}$, which was determined to be $1.20658 \times 10^{-5} \pm 5.01767 \times 10^{-8}$ GeV^{-2}.

Comparing the two trial Tau values directly, as opposed to averaging them, yields a 0.51% difference. This difference is quite small, which indicates that systematic error, if it is even present, is also very small. A similar procedure was conducted with our calculated values for τ and $G_F^{\,o}$, and it was determined that our τ value differs from its commonly accepted value of 2.19698 microseconds (Zyla et al., 2021) by 7.49% and that our value for $G_F^{\,o}$ differs from its commonly accepted value of 1.16638×10^{-5}GeV^{-2} (Zyla et al., 2021) by 3.33%. These differences can be explained by the fact that our value for τ is an *average* of the lifetimes of positively charged and negatively charged muons.

As explained in the introduction, positively charged muons have only one decay mode: spontaneous decay via the weak force. Negatively charged muons also decay this way, but they can also decay via muon capture with one of the scintillator atoms. The fact that negatively charged muons also have this additional decay mode increases their probability of decaying, thereby shortening their average lifetime by some amount. Our experiment had no way to distinguish between the decays of negatively charged muons and positively charged muons, so the calculated muon lifetime is really just an average of the two. Consequently, this average is somewhat smaller than that of a muon in free space (where muon capture cannot occur) because the negative muons' shorter lifetime weighs it down.

The accuracy of this experiment could therefore be improved if a method could be found, either via a change in the apparatus itself or via some statistical technique, that would

enable the lifetimes of positively and negatively charged muons to be measured separately. Being able to measure these two quantities separately would not only allow us to learn more about the mechanism of muon capture, but would yield a much more accurate value for τ, as the average lifetime of a positively charged muon (with its single decay mode) is simply equivalent to the average decay of a muon in free space.

Putting aside the slight inaccuracy of our τ value, the result is still close enough to the accepted value to serve as qualitative evidence for relativistic time dilation. As discussed in the introduction, the muons studied in this experiment are produced at an altitude of approximately 15 kilometers above sea level. These muons have an average total energy of about 4 GeV (3.894346 GeV of kinetic energy), which can be used in conjunction with Equation 4.1 (Harris, 2008) to determine their average velocity.

$$KE = m_{\mu}c^{2}\left(\frac{1}{\sqrt{1-\frac{v^{2}}{c^{2}}}} - 1\right) \quad (4.1)$$

Solving this equation for v, the velocity, and plugging in the muon mass and kinetic energy yields a velocity of 0.996c. Even traveling at this great speed, it would still take a muon 50.05212 microseconds to travel a distance of 15 kilometers. As we've determined, a muon only lives for approximately two microseconds, meaning that it would be impossible for the muon to travel this far *unless* it experiences relativistic time dilation. Thus, the muon's short lifetime is a great example of the fact that, as predicted by special relativity, fast moving objects experience time more slowly when viewed from a reference frame moving slowly relative to that of the object.

5

Bibliography

Brown, G. (2022). *Physics 134 Lab Manual*, 39 - 42.

Coan, T., & Ye, J. (2005). *Muon Physics*.

Harris, R. (2008). *Modern Physics* (Vol. 2), 34.

Zyla et al. (2021), Muon Information, Physical constants, *2021: Particle Listings.* Retrieved April 15, 2022, from https://pdg.lbl.gov/2021/listings/contents_listings.html